

PROCEEDINGS



SPIE—The International Society for Optical Engineering

Microelectronic Processes, Sensors, and Controls

James A. Bondur
Kiefer Elliott
John R. Hauser
Dim-Lee Kwong
Asit K. Ray
Chairs/Editors

27–29 September 1993
Monterey, California

Sponsored and Published by
SPIE—The International Society for Optical Engineering



Volume 2091

SPIE (The Society of Photo-Optical Instrumentation Engineers) is a nonprofit society dedicated to the advancement of optical and optoelectronic applied science and technology.

ELECTRICAL SENSORS FOR MONITORING RF PLASMA SHEATHS

Mark A. Sobolewski and James K. Olthoff

National Institute of Standards and Technology
Gaithersburg, MD 20899

ABSTRACT

We have investigated the use of radio-frequency (rf) current and voltage measurements to monitor the electrical characteristics of rf plasmas and to predict changes in ion kinetic energy distributions. These studies were performed at 2.7 and 13.3 Pa (20 and 100 mTorr) in a Gaseous Electronics Conference (GEC) RF Reference Cell in mixtures of argon with oxygen, nitrogen and water. The relative concentrations of oxygen, nitrogen and water were varied from below 0.01% to over 10%. Simultaneous with the electrical measurements, the kinetic energy distributions of ions at the grounded electrode were obtained using a mass spectrometer equipped with an ion energy analyzer. As operating conditions were varied, the mass spectrometer revealed changes in the maximum ion energy that paralleled changes in the electrical measurements. The electrical data were sensitive to concentrations of oxygen < 0.01% (and also to small quantities of nitrogen and water) suggesting that careful attention to background gases is necessary to assure the greatest reproducibility of plasma conditions. In addition, in argon/oxygen mixtures at 2.7 Pa, the electrical measurements revealed slow changes that we believe are caused by increases and decreases in the quantity of oxygen adsorbed on the surface of the cell's aluminum electrodes. It is expected that the measurement techniques described here could be extended to monitor the sheath above a wafer during plasma etching to obtain information about changes in the condition of the wafer surface and the energies of ions bombarding it.

1. INTRODUCTION

Plasma etching is widely used in semiconductor processing due to its unique ability to etch anisotropically, producing features with steep walls and trenches with high aspect ratios. The origin of the anisotropy lies in the directed motion of ions towards the wafer to be etched. Ions are accelerated by electric fields in the plasma sheath, a dark, electron-free region located between the plasma glow and the wafer surface. Thus the electrical properties of the sheath play a fundamental role in the mechanism of plasma etching. In particular, the voltage drop across the sheath plays a dominant role in determining the kinetic energy that an ion will have when it strikes the wafer surface, and this energy is in turn an important factor in determining the etch rate and the severity of sputter damage. Also, the sheath electrical properties determine whether thin gate oxides will be degraded by charging damage during plasma processing¹ and whether electrically charged dust particles generated in the plasma will traverse the sheath and contaminate the wafer. For all these reasons, the electrical properties of plasma sheaths are critical process parameters in plasma etching.

Measurements of the voltage and current in the electrical circuit that powers the plasma cell can provide electrical and physical information about the plasma and its sheaths. Sometimes these measurements are used simply to detect changes in the discharge with no attempt made to interpret them. As such, the measurements are a useful means of gauging the reproducibility of conditions in several identical cells^{2,3} and the sensitivity of the conditions in a single cell to changes in its external powering circuitry.^{4,5} Furthermore, when changes in electrical measurements are correlated with physical processes occurring in the plasma, they can be used to monitor or detect these processes. One example of this is electrical detection of etching endpoints.^{6,7} Finally, when current and voltage measurements are combined with models of the electrical behavior of the discharge, one can obtain values for relevant plasma parameters such as electron density,^{8,9,10} sheath thickness,^{11,12,13} sheath electric field,¹⁴ and ion bombardment energies.^{15,16} However, further application of these efforts requires development of more sophisticated and more general models of the electrical behavior of discharges and wider testing of these models by experiment.

A particularly important area where further research is needed involves the relationships between voltages measured externally, the voltage drops across plasma sheaths, and the kinetic energies of ions accelerated across them. This study concentrates on an investigation of these relationships. We measured the current and voltage

waveforms on the powered electrode of an rf parallel-plate discharge cell and the kinetic energy distributions of ions incident on the grounded electrode. Data obtained over a wide range of conditions were compared in order to test the ability of the electrical data to predict changes in the ion energy distributions. Plasmas were generated at 2.7 and 13.3 Pa (20 and 100 mTorr) in mixtures of argon gas with oxygen, nitrogen and water. Argon is an electropositive gas and the addition of even small quantities of electronegative gases should produce significant changes in both the electrical behavior of the discharge and the ion energy distributions.¹⁷ We varied the concentrations of oxygen, nitrogen and water from below 0.01% to above 10%. Low concentrations were of interest because these three gases are all common contaminants in plasma systems. We wondered if contamination by these gases could have been a source of irreproducibility in previous electrical measurements of argon discharges or of disagreements between theory and experiment.

In this study we found that certain electrical measurements were correlated to changes in the kinetic energies of the most energetic ions. In addition, for mixtures of argon and oxygen at 2.7 Pa, we observed slow, time-dependent changes in the electrical measurements that we attribute to changes in the quantity of oxygen adsorbed on the surface of the cell's aluminum electrodes. In sum, this work illustrates the utility of electrical measurements for sensing changes in both ion energies and surface conditions, and may hasten the development of theoretical understanding of the electrical characteristics of discharges and further applications of the electrical measurements as a tool for monitoring plasma processing.

2. EXPERIMENTAL APPARATUS

Experiments were performed in a GEC reference cell,^{2,3,18} a standard cell designed to facilitate direct comparison of experimental results obtained in different laboratories. The cell has two aluminum electrodes with diameters of 10 cm, separated by a gap of 2.54 cm. The grounded upper electrode was modified to incorporate a Hiden EQP Plasma Probe mass spectrometer¹⁹ described in detail elsewhere.²⁰ This spectrometer is equipped for ion energy analysis and also has an electron impact ionizer. The ionizer generates 70 eV electrons to ionize neutral species, allowing the spectrometer to act as a residual gas analyzer. Ions and neutrals enter the spectrometer through a 0.1-mm hole in the center of the upper electrode. This electrode is supported by a 10-cm-diameter stainless steel tube that also serves to ground it to the vacuum chamber. In contrast, an Al₂O₃ ceramic piece supports the powered lower electrode and provides it with electrical insulation from its stainless steel ground shield and the chamber. The lower electrode was driven at 13.56 MHz by an ENI ACG-5 power supply¹⁹ coupled through a 0.1 μ F blocking capacitor and an isolating rf filter.^{4,5} No matching network was used. The lower electrode is equipped for water cooling, but at the low power levels of these experiments water cooling was not necessary and was not used.

Argon gas (99.999% purity) was supplied to the cell through a showerhead arrangement of many small holes in the powered lower electrode, at a flow rate of 1.7×10^{-2} Pa m³/s (10 sccm). Oxygen and nitrogen were supplied through a second gas line, equipped with a leak valve and an isolation valve, which joined the argon line at the cell. Water vapor was supplied through the same valves, from a closed reservoir. Prior to argon/water experiments, air and dissolved gases were removed from the reservoir by cooling it below 0°C and then opening the valves between it and the system's high vacuum turbo pump. We repeated this freeze/pump/thaw cycle several times. During argon/water experiments, the leak valve was heated to prevent flow instabilities that arise from condensation of water inside the leak valve.

The cell was equipped with two separate pumping systems. At 13.3 Pa, gas flowed out of the cell to a mechanical pump through six symmetrically placed holes in the base of the reactor. A constant pressure was maintained in the cell by a throttle valve in the exhaust line controlled by a signal from a capacitance manometer. In contrast, at 2.7 Pa gas was exhausted through a 6" side port to a turbo pump, and the pressure was maintained by manually varying the speed of the turbo pump.

3. ELECTRICAL MEASUREMENTS

A Pearson model 2877 current probe¹⁹ and a Hewlett Packard 10430A 10:1 attenuating voltage probe¹⁹ were attached to the power lead downstream of the blocking capacitor, as close as possible to the powered electrode. A

Hewlett Packard 54503A oscilloscope¹⁹ digitized the probe signals and transferred the digital data to a computer which extracted the amplitudes and phases of the significant Fourier components using an iterative least squares curve fitting algorithm.¹⁴ Each fit included a dc component, the fundamental (13.56 MHz) component and the second through fifth harmonics. Phases obtained from the fits were then corrected to account for propagation delays in the cables connecting the probes to the oscilloscope. Corrections for the effects of parasitic stray capacitance and series inductance in the powered electrode assembly were also made, using a technique²¹ that requires no assumptions about the parasitics. To improve the precision of the corrected results, an inductive shunt circuit^{2,3,5,21} was connected between the power lead and the chamber ground, downstream of the current probe, and it was adjusted to null the parasitic current at 13.56 MHz.

By this process, we convert the voltage and current waveforms measured by the probes into the waveforms $V(t)$ and $I(t)$ present on the powered electrode. $I(t)$ represents the current flowing from the surface of the powered electrode into the plasma, and $V(t)$ represents the voltage between the powered electrode and its ground shield. This is not exactly the same as the voltage between the electrodes, as parasitic inductance in the ground connections between this shield and the grounded electrode produces a voltage drop between them. Nevertheless, we have measured this inductance and found it to be sufficiently low that the rf voltage difference between the grounded electrode and the ground shield of the powered electrode would be < 1 V for the frequency and current levels at which we operated. Thus $V(t)$ is very nearly the voltage between the electrodes, and we will treat it as such below.

Several different voltage drops across distinct regions of the plasma contribute to $V(t)$. These include a drop across the sheath at the powered electrode, a smaller voltage drop across the glow region of the plasma, and another drop across the sheath at the grounded electrode. The voltage drop across each sheath varies with time as the sheath expands and collapses during each rf cycle. Ideally, one would want to know the time-dependent values of the sheath voltages individually, but this requires more information, either from additional experimental measurements or from a model of the electrical behavior of the plasma. Nevertheless, if certain reasonable assumptions are made, an estimate of the peak-to-peak value of the sheath voltages can be obtained.^{14, 22} The assumptions are that the voltage drop across the glow is negligibly small, that the two sheaths oscillate 180° out of phase, and that the voltage drop across the ground sheath, when it is fully contracted, is the same as the drop across the fully contracted powered sheath. Given these assumptions, the peak-to-peak value of the ground sheath voltage drop can be shown to be equivalent to V_{\max} , the highest value attained by the waveform $V(t)$. The absolute value of V_{\min} , the minimum waveform voltage, provides a value for the peak-to-peak amplitude of the powered sheath voltage. Measurements of V_{\max} and V_{\min} can thus be used to determine the sensitivity of the sheath voltage drops to perturbations of the plasma. For example, when the voltage applied to argon discharges is changed, V_{\min} changes while V_{\max} remains constant, indicating that only the powered sheath, not the ground sheath, responds to this change.¹⁴ Finally, as the voltage drop across a sheath varies, the acceleration experienced by ions in that sheath will also vary. Thus, changes in V_{\max} and V_{\min} can be used to detect changes in the kinetic energies of ions striking the grounded and powered electrodes, as demonstrated below.

4. ELECTRICAL RESULTS AT 13.3 PA

Electrical data measured at 13.3 Pa (100 mTorr) are shown in Fig. 1. In three separate experiments, O_2 , H_2O and N_2 were added to the argon plasma in varying amounts, using the leak valve. During the experiments, the mass spectrometer was operated as a residual gas analyzer to monitor neutral species in the plasma. The count rates at masses 32, 18 and 28 (measured with the plasma ignited, simultaneous with the electrical measurements) were converted to the values of O_2 , H_2O and N_2 concentration shown on the x axes. These values, representing the concentration of each species relative to argon, were obtained as follows. First, we subtracted a background count rate to account for residual gases in the differentially-pumped mass spectrometer chamber. The difference was then divided by the count rate of the argon isotope at mass 36 to account for any changes in the efficiency of the electron-impact ionizer over time. Such changes affect all mass species equally, so they are canceled out by this normalization. The resulting ratios were then converted to relative concentrations by a calibration factor obtained using the capacitance manometer. Separate calibrations were performed for each gas. During calibrations, the feedback loop controlling the pressure was disabled and the exhaust valve set to a fixed position. While the argon flow was maintained, the flow of the second gas (O_2 , H_2O or N_2) was interrupted by closing the leak and isolation

valves. Values of the count ratio and pressure measured with the valves open and closed yield the necessary calibration factor. Calibration factors obtained at varying concentrations (in the range 0.5-15%) were all in agreement. Calibrations repeated over many weeks also agreed well.

The electrical parameters on the y axes of Fig. 1 are derived from $V(t)$ and $I(t)$, the corrected voltage and current waveforms. As described above, V_{\max} is the highest voltage attained by $V(t)$ while V_{dc} and V_1 are the amplitudes of the dc and fundamental (13.56 MHz) components of $V(t)$. Also shown are the magnitude and phase of the impedance defined as V_1/I_1 , where I_1 is the fundamental component of $I(t)$. At concentrations as low as 60 ppm O_2 , 200 ppm H_2O and 600 ppm of N_2 , significant changes in these parameters were observed, illustrating how sensitive argon discharges can be to small concentrations of these common impurities. In this paper, we concentrate on the changes in V_{\max} and V_{dc} , but the impedance changes are also important. The impedance data contains additional information about the mechanisms of power dissipation in the discharge.^{10-13, 24, 25} But it is difficult to obtain such information when many different dissipation mechanisms are present simultaneously, as simulations suggest.²⁶

Despite changes in the impedance of the plasma, the rf power supply was able to maintain a rather stable output voltage without requiring readjustment. Thus, V_1 remained relatively constant throughout the experiments, and so did V_{pp} , the peak-to-peak amplitude of $V(t)$. Because the amplitudes of the harmonic components of $V(t)$ were relatively small, $V_{\text{pp}} \approx 2V_1$ and $V_{\max} \approx V_1 + V_{\text{dc}}$. Thus, with V_1 constant, the changes in V_{\max} and V_{dc} were approximately equal.

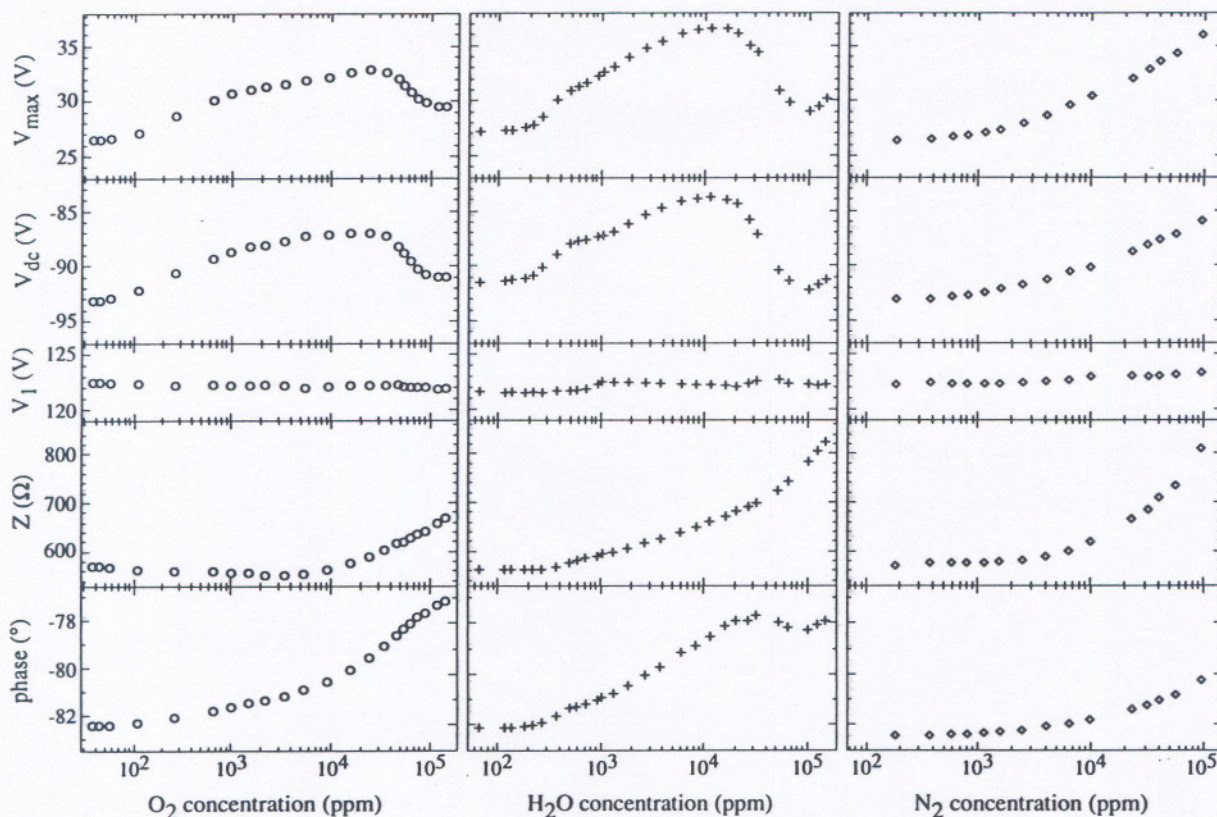


Fig. 1. Electrical data for Ar/O₂ (left), Ar/H₂O (center) and Ar/N₂ (right) plasmas at 13.3 Pa (100 mTorr). The relative concentrations in parts per million (ppm) given on the x axes were obtained from calibrated mass spectrometer measurements. The electrical parameters on the y axes include: V_{\max} , the maximum value attained by the corrected voltage waveform $V(t)$; V_{dc} and V_1 , the dc and fundamental (13.56 MHz) components of $V(t)$; and the magnitude (Z) and phase of the impedance V_1/I_1 , where I_1 is the fundamental current component.

V_{\max} and V_{dc} rose with increasing O_2 or H_2O concentrations up to 1-2%, but at higher concentrations they fell. This reversal may be related to the production of negative ions in the bulk plasma which would act to lower the plasma potential, thus reducing the sheath voltage drops and the parameter V_{\max} . Negative ions should be less prevalent in Ar/ N_2 mixtures, as N_2 has relatively low attachment rates.²³ Therefore it is not surprising that only a monotonic rise in V_{\max} and V_{dc} is observed for Ar/ N_2 . The rise in V_{\max} and V_{dc} , seen for all three mixtures, is not presently understood. Nevertheless, the changes in V_{\max} in both directions were correlated to changes in the ion energy measurements presented below.

To study the chemical reactions induced by the plasma, we turned the discharge off periodically throughout these experiments, while we continued to acquire mass spectrometer data. Typically, the count rate of whichever gas we were adding to argon increased when the plasma was extinguished (and decreased again when the plasma was re-ignited) indicating that some fraction of the O_2 , N_2 or H_2O flowing into the cell was dissociated within the plasma. Species produced in the plasma behave in the opposite fashion; when the discharge is turned off their count rates fall. For example, when Ar/ O_2 or Ar/ H_2O discharges were turned off, the count rate of mass 44 and 28 neutrals fell, indicating that oxygen radicals produced by the plasma decomposition of O_2 and H_2O were reacting with some source of carbon (presumably pump oil) to produce CO_2 and CO. (Here, the mass 28 signal represents CO, not N_2 , as cracking of N_2 in the mass spectrometer would produce a corresponding N signal at mass 14, which was not observed.) The plasma dissociation of H_2O also produced O_2 ; in Ar/ H_2O plasmas, we observed significant O_2 concentrations that eventually reached 0.1% at the highest H_2O concentrations shown in Fig 1. When the Ar/ H_2O discharges were turned off the O_2 counts fell to background levels. Small declines in O_2 counts were observed when pure argon plasmas were extinguished, indicating that O_2 was produced in these plasmas, presumably from sputtering of oxygen previously adsorbed on surfaces within the cell. Additional evidence of reactions of O_2 with surfaces was obtained at lower pressures, as described below.

5. ELECTRICAL DATA AT 2.7 PA

Electrical measurements of Ar/ O_2 plasmas at 2.7 Pa (20 mTorr) are shown in Fig. 2 as a function of O_2 concentration. The experimental procedures were the same as at 13.3 Pa, with one exception: this time the vacuum was maintained by a variable-speed turbo pump rather than the throttled mechanical pump. Consequently, we used a different calibration method, in which the O_2 flow was shut off and the Ar flow was then increased to maintain the turbo pump at the same speed of rotation. The change in argon flow divided by its initial flow yielded the values for O_2 relative concentration shown on the x axis. This procedure is less accurate than the 13.3 Pa calibration method, and strictly speaking it provides a calibrated flow ratio, rather than a ratio of partial pressures.

The data in Fig. 2 display a surprising degree of hysteresis. In one experiment, shown in Fig. 2a, a constant flow of O_2 was abruptly introduced into an argon discharge and maintained for 40 min. Then the flow was shut off and the plasma was monitored for an additional 50 min. Seconds after initiating the flow, the O_2 concentration in the cell jumped to ~0.5%, but V_{dc} and the other electrical parameters responded much more slowly to this change. V_{dc} required 30 min to stabilize at a new, higher value. Similarly, when the O_2 flow was stopped, a rapid fall in O_2 concentration was observed over several seconds, a time scale consistent with the residence time of gas in the chamber. But V_{dc} required 40 min to fall back to its original value.

We believe that the slow upward drift in V_{dc} arises from the development of an oxygen-rich layer on the surface of one or both aluminum electrodes — either a layer of physisorbed oxygen or else an oxide layer formed by chemical reaction. Interestingly, as V_{dc} rises there is a simultaneous slow rise in O_2 concentration, producing a positive slope in this portion of the hysteresis curve. This increasing gas-phase O_2 concentration can be explained by a decreasing loss of gas-phase O_2 to the surface, as the oxygen-rich surface layer develops. Apparently, the development of the surface layer is self-limiting. By the time that V_{dc} stabilizes the layer has presumably reached its limiting thickness.

Conversely, the slow decline in V_{dc} after the O_2 flow is turned off can be explained by ion milling of the oxygen-rich surface layer as it is bombarded by argon ions. An alternate explanation is that this layer is not removed but is covered by aluminum sputtered off of the opposing electrode. However, this second hypothesis does not explain

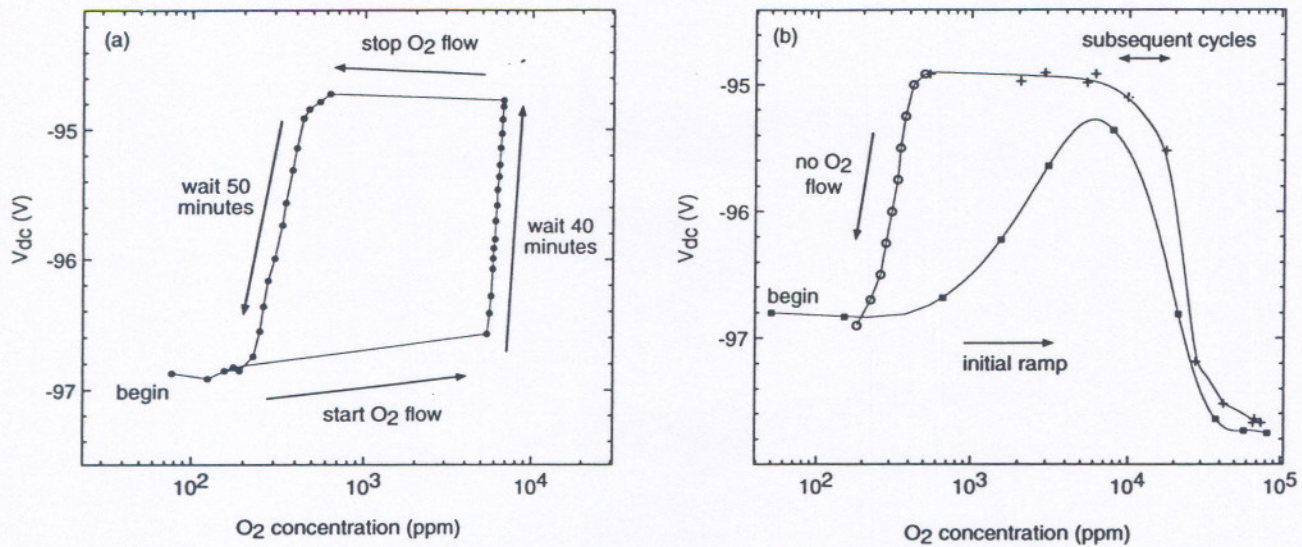


Fig. 2. V_{dc} , the dc component of the voltage waveform, for Ar/O₂ mixtures at 2.7 Pa (20 mTorr). In one experiment (a) a constant O₂ flow was turned on and then shut off 40 min later. In another (b) the O₂ concentration was first ramped to ~10% (■), then cycled between 0.1 and 10% (+), and then the O₂ flow was stopped while we continued to measure V_{dc} for a period lasting 50 min (o). The hysteresis in the data arises from the slow formation of an oxygen-rich layer on the surface of the aluminum electrodes, and a subsequent slow removal of the layer by sputtering.

the O₂ concentrations observed after the oxygen flow was shut off. After the initial, rapid decline, a slow decline from 600 to 200 ppm was observed. Presumably, this O₂ signal arises from oxygen sputtered off of surfaces. The flux of oxygen from a surface will decline as it is sputtered clean, resulting in the observed slow decrease in gas-phase O₂ concentration. Plasma must be present to observe this signal; in subsequent experiments the discharge was turned off during this part of the hysteresis cycle and the O₂ signal fell rapidly to background levels.

The slow surface-dependent changes in Fig. 2a may be analogous to changes in V_{dc} observed at the endpoint of plasma etches^{6,7} and may originate from changes in the emission of secondary electrons from the electrode surfaces. Because secondary electron emission is a very surface-sensitive property, a very thin oxygen-rich layer, possibly only a monolayer thick, could have measurable effects. It is interesting that evidence for sputtering of O₂ from surfaces was obtained at 13.3 Pa, as described above, but the hysteresis effects that dominate Fig. 2 were not observed. This suggests that changes in surface conditions still occur at 13.3 Pa, but the electrical characteristics are less sensitive to these changes. Indeed, a previous study has shown that the impedance of argon discharges at pressures ≥ 13.3 Pa is not very sensitive to changes in the electrode surface.¹² Excitations in the plasma glow are more important at higher pressures¹² and they may dominate the effects of secondary electrons.

Fig. 2b reveals additional effects at higher O₂ concentrations. In this experiment the O₂ concentration was first ramped (in staircase fashion) to about 10%. During this initial ramp V_{dc} rose, reached a maximum at around 1% O₂, and then fell. This behavior results from a combination of the slow time-dependent rise in V_{dc} related to surface conditions (as in Fig. 2a) and a fall in V_{dc} at higher O₂ concentrations. The fall in V_{dc} , also observed for high O₂ and H₂O concentrations at 13.3 Pa (Fig. 1), is presumably a gas-phase effect, related to the production of negative ions in the plasma glow. We then cycled the O₂ concentration down to 0.1% and back up to 10%. During this part of the experiment (labelled "subsequent cycles") the electrical parameters were functions solely of the O₂ concentration at the time of the measurement. Data from different cycles were in agreement. There were no time-dependent effects. This is presumably because the oxygen-rich surface layer had reached a self-limiting thickness near the end of the initial ramp in O₂ concentration. Finally, we shut off the oxygen flow and observed a slow recovery of the electrical parameters lasting 50 min which is again explained by removal of the surface layer by sputtering, as in Fig. 2a.

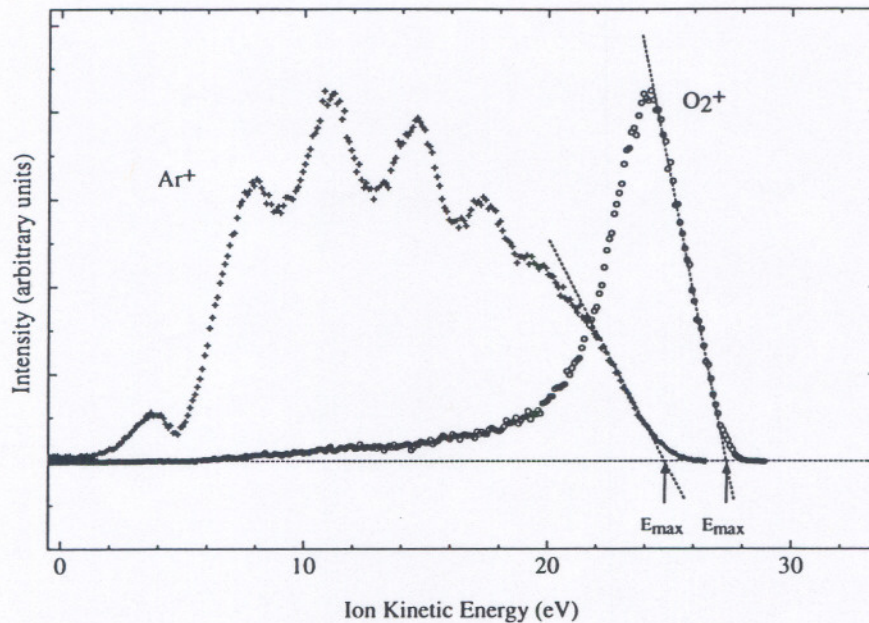


Fig. 3. Ion kinetic energy distributions for Ar^+ ions (+) and O_2^+ ions (o). The extrapolations used to define E_{max} , the maximum energy of each distribution, are also shown. The data was measured in a mixture of 2% O_2 in argon, at 13.3 Pa, with $V_1=122$ V.

6. COMPARISON WITH ION ENERGY DISTRIBUTIONS

We did additional experiments to see if the changes in V_{max} observed in Figs 1 and 2 were correlated with changes in the energies of ions bombarding the grounded electrode. We are primarily interested in the highest energy ions: ions formed in the glow that accelerate across the sheath without losing energy to collisions. The highest energy ions are often the most important in etching and damage processes.²⁷ Moreover, it is the energy of these ions that should be most closely correlated to the sheath voltages and the electrical parameter V_{max} . Ions that lose energy via collisions in the sheath or are formed in the sheath will have lower energies that would be more difficult to relate to the electrical measurements.

Because we were primarily interested in the highest energy ions, we extracted from each distribution a maximum kinetic energy E_{max} . To define this energy, the sharp drop at the high energy end of each distribution was linearly extrapolated, as shown in Fig. 3. The x-intercept of the extrapolation defines E_{max} . A small amount of signal was observed at energies above this, because the energy resolution of the spectrometer is not perfect.

The Ar^+ and O_2^+ ion energy distributions shown in Fig. 3 were measured for a 13.3 Pa Ar/O_2 plasma at an oxygen concentration of 2%. The O_2^+ distribution is relatively sharp, but broadening and multiple peaks are observed in the Ar^+ distribution. These features, also observed in pure argon discharges, are caused primarily by symmetric charge-exchange collisions in the sheath.^{20, 28} They are not observed in the O_2^+ distribution, because, at such a low oxygen concentration, the probability of an O_2^+ ion encountering an O_2 neutral in the sheath is relatively small. At higher O_2 concentrations, however, multiple peaks do appear in the O_2^+ distributions. Similarly, in $\text{Ar}/\text{H}_2\text{O}$ mixtures at 13.3 Pa, the distribution of H_2O^+ ions exhibit such features only at high H_2O concentrations. In contrast, in Ar/N_2 mixtures N_2^+ ions showed evidence of collisions in the sheath even at low concentrations of N_2 . In all cases, the Ar^+ distributions were broad at 13.3 Pa. However, when the pressure is lowered, the probability of collisions decreases, and the multiple peaks disappear. At 2.7 Pa the ion energy distributions of Ar^+ , O_2^+ and N_2^+ each show only a single, narrow peak. As the gas mixture was varied at 2.7 Pa, the distributions did not broaden or change in shape, and so shifts in E_{max} at this pressure closely tracked shifts in the mean ion energies.

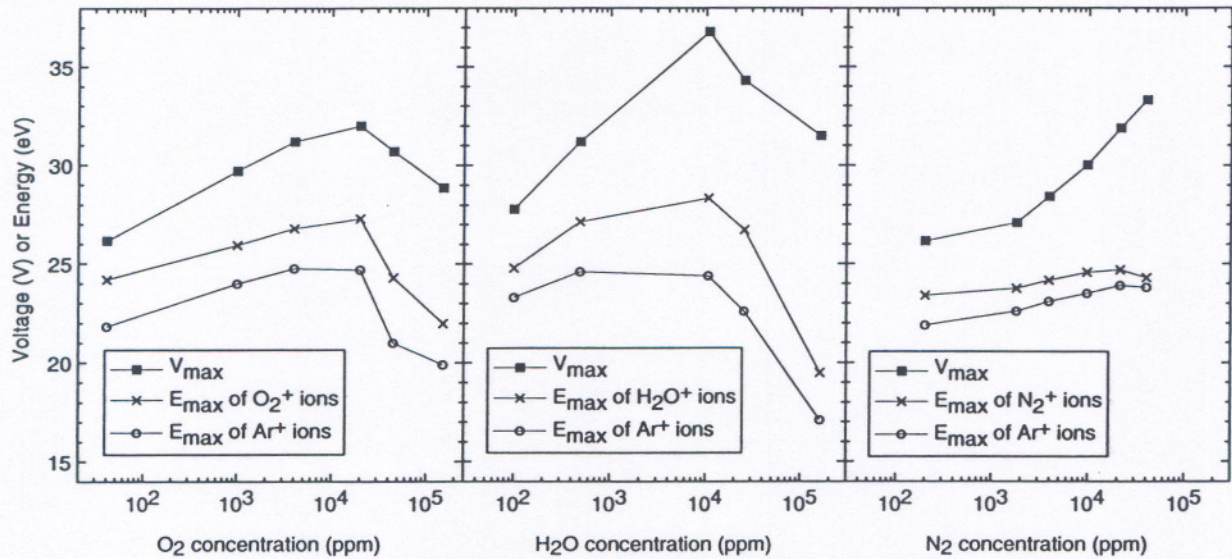


Fig. 4. Comparison of the maximum waveform voltage V_{\max} (in V) with E_{\max} (in eV) for Ar/O₂ (left), Ar/H₂O (center) and Ar/N₂ (right) plasmas at 13.3 Pa (100 mTorr). E_{\max} is the maximum ion kinetic energy as defined in Fig. 3. The relative concentration values on the x axes are estimates obtained from simultaneous measurements of the impedance and the previously measured relations between impedance and concentration shown in Fig. 1.

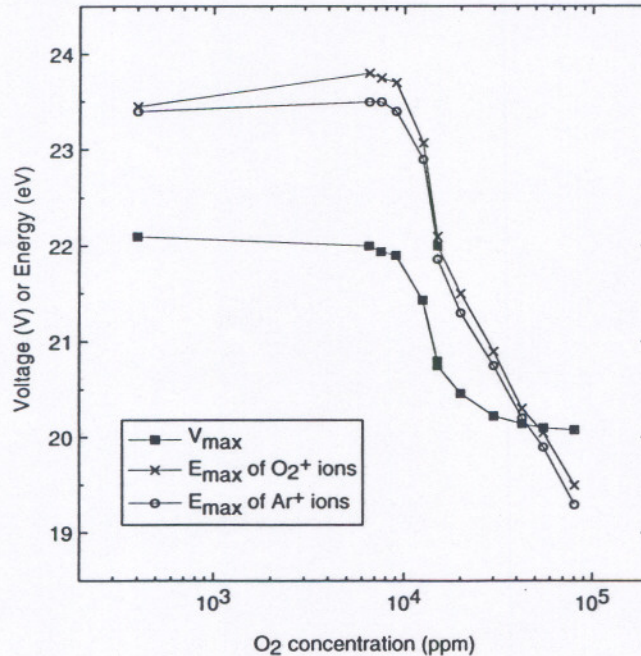


Fig. 5. Comparison of the maximum waveform voltage V_{\max} (in V) with E_{\max} (in eV) for Ar/O₂ mixtures at 2.7 Pa (20 mTorr). Here, the flow of O₂ as well as Ar was controlled by mass flow controller and the ratio of the flow readings were used to define the concentration values on the x axis. Prior to acquiring the data, an oxygen-rich plasma was sustained long enough to fully oxidize the surface of the aluminum electrode, so the data displays no hysteresis.

Values of the maximum kinetic energy E_{\max} are compared with the parameter V_{\max} in Fig. 4 for Ar/O₂, Ar/H₂O and Ar/N₂ mixtures at 13.3 Pa. During these experiment, the mass spectrometer remained in energy analysis mode, with the electron-impact ionizer turned off. Count rates for neutral species were not measured. Instead, the concentration values on the x axis were estimated from simultaneous measurement of the impedance magnitude and its previously measured dependence on concentration, given by Fig. 1.

In Fig 4, a qualitative agreement between the changes in V_{\max} and the changes in E_{\max} is observed. In all cases, the initial increase in V_{\max} occurs simultaneously with an increase in E_{\max} . When V_{\max} starts to decrease at 2% O₂ in Ar and at 1% H₂O in Ar, the E_{\max} values also begin to decrease. The slopes of the initial increases in E_{\max} are smaller than the slopes seen in V_{\max} , while at higher concentrations the decreases in E_{\max} are more rapid than decreases in V_{\max} . In Ar/N₂ mixtures the total increase in E_{\max} is small, ~1 Volt. While this increase levels off at high N₂ concentrations, the plot of V_{\max} shows positive curvature.

While V_{\max} is an estimate of the peak-to-peak amplitude of the ground sheath voltage, the maximum kinetic energy E_{\max} is more closely related to the time-averaged value of the sheath voltage. These relatively heavy ions have a plasma frequency lower than 13.56 MHz, and therefore they do not readily respond to the rf fields in the sheath. Electrical models²² relate the time-averaged and peak-to-peak value of the ground sheath potential, but we know of no fundamental reason why they should be equal. Thus changes in V_{\max} should be correlated to changes in E_{\max} , as observed, but there is no reason to expect them to exactly coincide. Furthermore, the accuracy of the V_{\max} values shown is rather limited, as V_{\max} is essentially given by the difference between two larger numbers, V_{dc} and V_1 . Systematic errors of a few percent in either the dc or 13.56 MHz calibration of the oscilloscope or voltage probe would result in a shift of the V_{\max} curve up or down by several volts, although these errors would not noticeably change the shape of the curve.

Finally, Fig. 5 shows a comparison of V_{\max} and E_{\max} for Ar/O₂ mixtures at 2.7 Pa. In this experiment alone, the Ar flow was increased to 3.4×10^{-2} Pa m³/s (20 sccm) and a mass flow controller, rather than the leak valve, was used to control the O₂ flow. The O₂ concentrations were obtained from the flow ratios. At the start of the experiment the aluminum electrodes were fully oxidized by an oxygen-rich plasma so electrical data acquired thereafter did not suffer from the hysteresis seen in Fig. 2. In Fig. 5, as in Fig. 4, most of the trends revealed by the electrical measurement V_{\max} also appear in the E_{\max} values. An exception occurs at high O₂ concentrations, where the decline in V_{\max} levels off while the E_{\max} values continue to decline. Otherwise, the V_{\max} and E_{\max} curves are almost parallel. In other experiments, under conditions similar to the experiment of Fig. 2a, no change was observed in ion energies measured simultaneously with the slow surface-dependent changes in the electrical measurements. Thus at 2.7 Pa, the electrical measurements were sensitive both to fast changes in gas-phase composition that perturbed the ion energies, as well as slow, surface-dependent changes that did not.

7. CONCLUSIONS

We have found that argon discharges are sensitive to small concentrations of the common contaminant gases O₂, N₂, and H₂O and to changes in surface conditions, specifically increases and decreases in the quantity of oxygen adsorbed on the surface of the cell's aluminum electrodes. Electrical measurements can be used to detect these changes and to predict, to some extent, how sheath voltage drops and ion kinetic energies will respond to them. In particular, a correlation was found between the electrical measurements and the kinetic energies of the most energetic ions, which are most important in sputter damage and plasma etching mechanisms. We do not currently fully understand the mechanisms that produce the changes in the electrical parameters and ion energies. More sophisticated models of the electrical behavior of rf discharges must be developed and tested experimentally before quantitative predictions of ion energies can be obtained from electrical measurements. Nevertheless, the correlation between the electrical measurements and ion energies means that the electrical measurements could prove immediately useful for monitoring plasma conditions in plasma etching applications, even without the development of additional models. Although we have only mentioned ions incident on the grounded electrode, the techniques described here are not limited to grounded substrates. Etching is also performed on wafers that are rf biased, both in parallel plate reactors and remote plasma sources, and we expect the electrical measurements to be equally useful in detecting changes in the kinetic energies of ions incident on these rf biased wafers.

8. REFERENCES

1. S. Fang and J. P. McVittie, "A model and experiments for thin oxide damage from wafer charging in magnetron plasmas," *IEEE Electron Device Lett.* **13**, 347 (1992).
2. P. J. Hargis Jr., K. E. Greenberg, P. A. Miller, J. B. Gerardo, J. R. Torczynski, M. E. Riley, G. A. Hebner, J. R. Roberts, J. K. Olthoff, J. R. Whetstone, R. J. Van Brunt, M. A. Sobolewski, H. M. Anderson, M. P. Splichal, J. L. Mock, P. Bletzinger, A. Garscadden, R. A. Gottscho, G. Selwyn, M. Dalvie, J. E. Heidenreich, J. W. Butterbaugh, M. L. Brake, M. L. Passow, J. Pender, A. Lujan, M. E. Elta, D. B. Graves, H. H. Sawin, M. J. Kushner, J. T. Verdeyen, R. Horwath and T. R. Turner, "The GEC RF Reference Cell: A defined parallel-plate radio-frequency system for experimental and theoretical studies of plasma-processing discharges," *Rev. Sci. Inst.* in press (1993).
3. K. E. Greenberg, P. J. Hargis Jr. and P. A. Miller, *The GEC Reference Cell: Diagnostic Techniques and Initial Results* (Sandia National Laboratories internal report SETEC 90-013, 1990).
4. P. A. Miller, H. Anderson and M. P. Splichal, "Electrical isolation of radio-frequency plasma discharges," *J. Appl. Phys.* **71**, 1171 (1992).
5. P. A. Miller, "Electrical characterization of rf plasmas," *Proc. SPIE* **1594**, 179 (1991).
6. K. Ukai and K. Hanazawa, "End-point determination of aluminum reactive ion etching by discharge impedance monitoring," *J. Vac. Sci. Technol.* **16**, 385 (1979).
7. S. C. McNevin, D. J. Vitkavage and C. N. Bredbenner, "Bias voltage diagnostics during oxide etch in Drytek 384T," *J. Vac. Sci. Technol. A* **11**, 1142 (1993).
8. J. W. Butterbaugh, L. D. Baston and H. H. Sawin, "Measurement and analysis of radio frequency glow discharge electrical impedance and network power loss," *J. Vac. Sci. Technol. A* **8**, 916 (1990).
9. B. E. Thompson and H. H. Sawin, "Polysilicon etching in SF₆ rf discharges: Characteristics and diagnostic measurements," *J. Electrochem. Soc.* **133**, 1887 (1986).
10. K. D. Allen, H. H. Sawin, M. T. Mocella and M. W. Jenkins, "The plasma etching of polysilicon with CF₃Cl/argon discharges: I. Parametric modeling and impedance analysis," *J. Electrochem. Soc.* **133**, 2315 (1986).
11. P. Bletzinger and M. J. Fleming, "Impedance characteristics of an rf parallel plate discharge and the validity of a simple circuit model," *J. Appl. Phys.* **62**, 4688 (1987).
12. P. Bletzinger, "Experimental characteristics of rf parallel plate discharges: Influence of attaching gases," *J. Appl. Phys.* **67**, 130 (1990).
13. C. Beneking, "Power dissipation in capacitively coupled rf discharges," *J. Appl. Phys.* **68**, 4461 (1990).
14. M. A. Sobolewski and J. R. Whetstone, "Electrical measurements for monitoring and control of rf plasma processing," *Proc. SPIE* **1803**, 309 (1992).
15. B. E. Thompson, K. D. Allen, A. D. Richards and H. H. Sawin, "Ion bombardment energy distributions in radio-frequency glow-discharge systems," *J. Appl. Phys.* **59**, 1890 (1986).
16. K. D. Allen and H. H. Sawin, "The plasma etching of polysilicon with CF₃Cl/argon discharges: II. Modeling of ion bombardment energy distributions," *J. Electrochem. Soc.* **133**, 2326 (1986).
17. A. P. Paranjpe, J. P. McVittie and S. A. Self, "Scaling laws for radio frequency glow discharges for dry etching," *J. Vac. Sci. Technol. A* **8**, 1654 (1990).
18. J. R. Roberts, J. K. Olthoff, R. J. Van Brunt and J. R. Whetstone, "Measurements on the NIST GEC Reference Cell," *Proc. SPIE* **1392**, 428 (1990).
19. The identification of commercial materials and their sources is made to describe the experiment adequately. In no case does this identification imply recommendation by the National Institute of Standards and Technology nor does it imply that the instrument is the best available.
20. J. K. Olthoff, R. J. Van Brunt, S. B. Radovanov, J. A. Rees and R. Surowiec, "Kinetic energy distributions of ions sampled from argon plasmas in a parallel-plate, radio-frequency reference cell," *J. Appl. Phys.* in press (1994).
21. M. A. Sobolewski, "Electrical characterization of radio-frequency discharges in the GEC Reference Cell," *J. Vac. Sci. Technol. A* **10**, 3550 (1992).
22. K. Kohler, J. W. Coburn, D. E. Horne, E. Kay and J. H. Keller, "Plasma potentials of 13.56 MHz rf argon glow discharges in a planar system," *J. Appl. Phys.* **57**, 59 (1985).

23. L. G. Christophorou, D. L. McCorkle and A. A. Christodoulides, "Electron Attachment Processes," in *Electron-Molecule Interactions and Their Applications*, L. G. Christophorou, ed., Vol. 1, pp. 580 (Academic Press, Orlando, 1984).
24. B. Andries, G. Ravel and L. Peccoud, "Electrical characterization of radio-frequency parallel-plate capacitively coupled discharges," *J. Vac. Sci. Technol. A* **7**, 2774 (1989).
25. A. J. Van Roosmalen, W. G. M. van den Hoek and H. Kalter, "Electrical properties of planar rf discharges for dry etching," *J. Appl. Phys.* **58**, 653 (1985).
26. P. Belenguer and J. P. Boeuf, "Transition between different regimes of rf glow discharges," *Phys. Rev. A* **41**, 4447 (1990).
27. B. Chapman, *Glow Discharge Processes* (Wiley, New York, 1980).
28. J. K. Olthoff, R. J. Van Brunt and S. B. Radovanov, "Ion kinetic energy distributions in argon rf glow discharges," *J. Appl. Phys.* **72**, 4566 (1992).